THE ASTROPHYSICAL JOURNAL, 429:L81–L84, 1994 July 10

VEGA: A RAPIDLY ROTATING POLE-ON STAR

AUSTIN F. GULLIVER
Department of Physics and Astronomy, Brandon University, Brandon, MB, Canada R7A 6A9
GRAHAM HILL
Dominion Astrophysical Observatory, 5071 West Saanich Road, Victoria, BC, Canada V8X 4M6
AND
SAUL J. ADELMAN[1]
Department of Physics, The Citadel, Charleston, SC 29409
Received 1993 December 3; accepted 1994 April 25

ABSTRACT

High-dispersion (2.4 Å mm^{-1}), ultrahigh signal-to-noise ratio (3000:1) Reticon spectra of Vega revealed two distinct types of profiles. The strong lines exhibit classical rotational profiles with enhanced wings, but the weak lines have distinctly different, flat-bottomed profiles. Using ATLAS9 model atmospheres and SYNTHE synthetic spectra, Vega has been modeled as a rapidly rotating, pole-on star with a gradient in temperature and gravity over the photosphere. By fitting to the flat-bottomed line profiles of Fe I λ4528 and Ti II λ4529, we find least-squares fit values of $V \sin i = 21.8 \pm 0.2$ km s^{-1}, polar $T_{\rm eff} = 9695 \pm 25$ K, polar $\log g = 3.75 \pm 0.02$ dex, $V_{\rm eq} = 245 \pm 15$ km s^{-1}, and inclination $5\overset{\circ}{.}1 \pm 0\overset{\circ}{.}3$. The variations in $T_{\rm eff}$ and $\log g$ over the photosphere total 390 K and 0.08 dex, respectively. Assuming $V \sin i = 21.8$ km s^{-1}, an independent fit to the observed continuous flux from 1200 to 10,500 Å produced a similar set of values with polar $T_{\rm eff} = 9595 \pm 20$ K, polar $\log g = 3.80 \pm 0.03$ dex, and inclination $6\overset{\circ}{.}0 \pm 0\overset{\circ}{.}7$.

Subject headings: stars: atmospheres — stars: early-type — stars: individual (α Lyrae)

1. INTRODUCTION

Astronomers have repeatedly studied Vega (α Lyrae = HD 172167 = HR 7001), arguably the next most important star in the sky after the Sun. It has been used extensively as a primary and secondary spectrophotometric standard in the near-infrared, optical, and ultraviolet regions (Hayes 1985; Bohlin et al. 1990) and as a comparison star for elemental abundance studies of A- and B-type stars. However, studies of its elemental abundances show that it is metal-weak by −0.6 dex (Adelman & Gulliver 1990) compared to the Sun. Infrared measurements indicate that it is surrounded by a circular shell or disk (Aumann et al. 1984). Further, its apparent diameter is larger than expected for a minimally rotating A0 V star (Hanbury Brown et al. 1967). Its weak line profiles as seen in high signal-to-noise (S/N) spectra are clearly flat-bottomed, resulting in a trapezoidal appearance, while the strong lines exhibit normal rotationally broadened profiles (Gulliver et al. 1991). Elste (1992) suggested that the differing profiles can be explained in principle by a center-to-limb variation of their equivalent widths plus a latitude-dependent photospheric structure.

Castelli & Kurucz (1994, hereafter CK) compared blanketed LTE models for Vega calculated with the new ATLAS9 and ATLAS12 codes (Kurucz 1993) with the observed energy distribution and Balmer line profiles. Their preferred model had $T_{\rm eff} = 9550$ K, $\log g = 3.95$, and a microturbulent velocity $\xi = 2$ km s^{-1} for a metallicity $[M/H] = -0.5$.

When one uses spectral synthesis techniques with their model, one finds that the weak lines do not have the observed profiles. To see whether we can explain the appearance of the weak lines as well as the observed disk, we turn to a possibility suggested by Gulliver et al. (1991), namely, that we are observing Vega nearly pole-on. Gray (1985, 1988) also proposed this possibility based upon Vega's excessive luminosity. In such a model we might expect that the flat-bottomed profiles would result from a temperature gradient over the photosphere due to its rapid rotation. Also, if the rotation is sufficiently rapid, the anomalous diameter and the presence of a shell are more plausible.

2. OBSERVATIONS

Vega was observed with the Dominion Astrophysical Observatory 1.2 m telescope using the coudé spectrograph and an 1872 pixel bare Reticon with 15 μm pixels. The portion of the spectrum of Vega discussed here extends from 4487 to 4553 Å in wavelength steps of 0.035 Å and has a mean S/N of 3300 for the continuum regions after the co-addition of two spectra. A scattered light correction of 4% (Fletcher 1990) was applied to the co-added spectrum. A digitized instrumental profile of the spectrograph plus Reticon was constructed by co-adding nine intensity-weighted lines from the comparison spectrum. The resultant FWHM was 0.081 Å. The comparison star, *o* Peg, which was treated in a similar manner, had a mean S/N of 750.

3. MODELING

As the first step in the modeling process, a grid of 63 ATLAS9 models was calculated from $T_{\rm eff} = 7500$ K to $T_{\rm eff} = 11{,}500$ K in steps of 500 K and from $\log g = 3.00$ to $\log g = 4.50$ in steps of 0.25 for a metallicity $[M/H] = -0.5$ and $\xi = 1$ km s^{-1}. These models used the improved continuum opacities, increased line opacities, and finer sampling of the latest opacity distribution functions of Kurucz (1993). The metallicity and microturbulence were chosen to ensure consistency between the available scaled solar abundance opacity distribution tables of Kurucz and the calculated model atmospheres. Although Adelman & Gulliver (1990) found a mean

[1] Guest Investigator, Dominion Astrophysical Observatory.

underabundance of -0.6 dex and $\xi = 0.6$ km s^{-1}, the abundance difference is less than the quoted errors, and the difference in microturbulence has negligible impact on the weak lines modeled here. Indeed, the synthetic profiles for the strong lines suggest that $\xi = 1.0$ km s^{-1} is more realistic.

For each $T_{\rm eff}$ and log g point in the above grid a synthetic intensity spectrum was calculated for $\lambda\lambda$4480–4580 using the SYNTHE program (Kurucz & Avrett 1981). The line parameters used were those provided with SYNTHE supplemented by the critically compiled iron peak gf-values of Fuhr, Martin, & Wiese (1988) and Martin, Fuhr, & Wiese (1988).

Since the model parameters would be dependent upon the gf-values, it was particularly important to establish these independently and as accurately as possible using the narrow-lined (V sin $i = 5.8$ km s^{-1}), A1 IV, slightly metal-rich star o Peg. To correct the significant discrepancies between the synthetic and observed line profiles, astrophysical gf-values were determined for 31 weak lines in the region from 4519 to 4540 Å. In adjusting the gf-values of the lines within this region, an ATLAS9 model was first calculated for $T_{\rm eff} = 9600$ K, log $g = 3.60$, and $\xi = 1$ km s^{-1} (Adelman 1988). Then repeated synthetic spectra were produced using the abundances of Adelman (1988), the gf-values being adjusted until a satisfactory fit was achieved.

Although the flat-bottomed, weak lines are observed throughout the spectrum of Vega (Gulliver et al. 1991), the region from 4519 to 4540 Å was selected because it contained the two best unblended examples, Fe I λ4528 and Ti II λ4529. Fortuitously, this same region also contains three examples of the normal, rotationally broadened profiles, Fe II λ4520, Fe II λ4522, and Ti II λ4534. Only Fe I λ4528 and Ti II λ4529 are used to model Vega, because the modeling process is extremely time-consuming and program array sizes already exceed 50 Mb.

Because of uncertainty in the value of ξ for o Peg, the gf-values of the three strong lines Fe II λ4520, Fe II λ4522, and Ti II λ4534 were adjusted to fit the observed Vega profiles using the model derived below, including $\xi = 1$ km s^{-1}. The adjustments for the tabulated values of the Fe II lines were small, -0.05 and -0.03 dex, respectively, while that for the Ti II line was relatively large at -0.34 dex.

Specific intensity line spectra were evaluated for the 17 values of $\mu = 1.0$ to 0.01 normally used in ATLAS9 and sampled every 0.01 Å from 4519 to 4540 Å for the 63 models. The variation in line strength with temperature can be demonstrated using the central intensity of the line profile at $\mu = 1.0$ (the variation with log g is negligible). In the top panel of Figure 1 this dependence is shown for log $g = 3.75$ for four lines. The rate of change of central intensity with $T_{\rm eff}$ determines whether a given feature in the spectrum of Vega will appear flat-bottomed or not. If Vega is a rapidly rotating, pole-on star, then there exists a temperature gradient from the hotter pole (near the center of the disk) to the cooler equator (near the stellar limb). For the weak lines the lower temperatures at the equator/limb result in an enhanced contribution to the outer edges of the profiles, i.e., a "limb strengthening." For the strong lines there is little variation in line strength with temperature. Moreover, from the greater slope for Fe I λ4528 compared with that for Ti II λ4529, the former can be expected to be a more sensitive indicator. These conclusions are confirmed in the bottom panel of Figure 1, in which the variation of equivalent width with μ is shown for the Vega model at inclination 0°.0 and an equator-on, slowly rotating model. The pole-on model is illustrated because equivalent

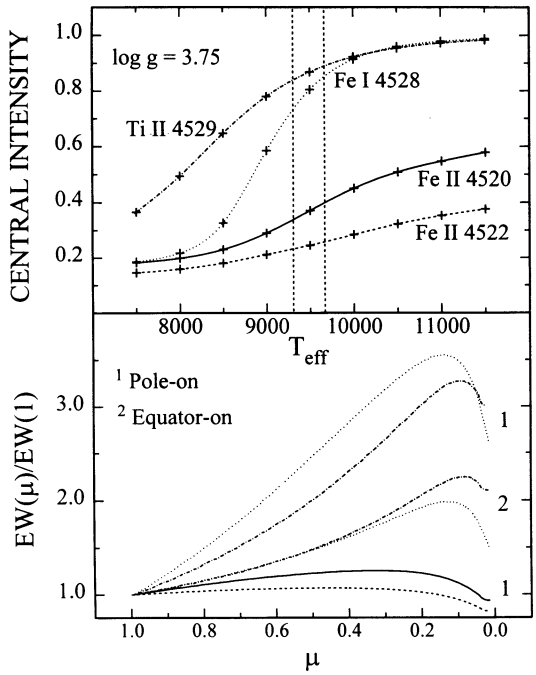

FIG. 1.—*Upper panel:* Variation in line profile central intensity at $\mu = 1.0$ with $T_{\rm eff}$ for the synthetic spectral features due to Fe II λ4520 (*solid line*), Fe II λ4522 (*dashed line*), Fe I λ4528 (*dotted line*), and Ti II λ4529 (*dash-dot line*) for log $g = 3.75$. The vertical lines indicate the model temperature limits. *Lower panel:* Variation of equivalent width with μ for the same lines, shown for a pole-on star (1) with polar $T_{\rm eff} = 9695$ K, polar log $g = 3.75$, and $V_{\rm eq} = 245$ km s^{-1} and an equator-on star (2) with $T_{\rm eff} = 9500$ K, log $g = 3.71$, and $V_{\rm eq} = 22.6$ km s^{-1} (only Fe I λ4528 and Ti II λ4529 are shown).

width is dependent only on μ. For the pole-on case the accentuation of the limb contribution for Fe I λ4528 and Ti II λ4529 is striking. The variation for Fe II λ4520 and Fe II λ4522 is much smaller and similar in both cases to the pole-on model shown.

For the analysis of the continuous energy distributions a separate input file of continuum specific intensity generated by ATLAS9 at the standard 17 values of μ from 1.0 to 0.01 and 1141 wavelengths from 506 Å to 160 μm for the 63 models was used. Either this continuous flux input file or the specific intensity line spectrum file is processed by a program, ROTATION, which generates a model having as free parameters V sin i, inclination, polar $T_{\rm eff}$, and polar log g. The line spectrum data is also convolved with a digitized instrumental profile. The physical model is based on the formulation given by Collins (1963). In performing the Gaussian quadrature, $T_{\rm eff}$, log g, and μ are calculated at each surface integration point with successive parabolic interpolations being performed to generate intensity as a function of wavelength. Initially a simple coarse grid search for a minimum in the mean square fit to the observations was made. Then, with these starting values, the routine CURFIT (Bevington 1969, p. 237) was used to minimize the mean square deviations.

To check the uniqueness of the adopted solution in each case, extensive grids were calculated to explore the multidimensional surface in detail. These grids were run for inclinations 3°–10°, polar $T_{\rm eff} = 9450$–9850 K, and polar log $g = 3.50$–4.20 with step sizes of 0°.1, 25 K, and 0.02 dex, respectively, assuming a constant V sin $i = 21.8$ km s^{-1}. These grid searches confirmed the validity of both solutions. They also

established that the solution derived from the line spectra was well determined but that from the continuous spectrum was less so.

4. RESULTS

Two nearly independent, similar solutions were found for the line spectrum and the continuous spectrum. The line spectrum produced the more definitive solution for a fit to the 4528–4530 Å region. A minimum of 2.54×10^{-7} in the mean square (observed minus calculated spectrum) deviation was found for the best-fit parameter values. Such a mean square deviation corresponds to a S/N of about 2000:1, about 60% of the observed S/N. The best-fit parameters were inclination 5°.1, polar $T_{\rm eff} = 9695$ K, polar $\log g = 3.75$, and $V \sin i = 21.8$ km s^{-1}. The mean values over the photosphere were $T_{\rm eff} = 9500$ K and $\log g = 3.71$, with equatorial minima of $T_{\rm eff} = 9300$ K and $\log g = 3.67$. The corresponding equatorial velocity was $V_{\rm rot} = 245$ km s^{-1}, with a ratio of equatorial to polar radii of 1.041. The continuous spectrum yielded a solution with a minimum of 8.05×10^{-5} with parameter values inclination 6°.0, polar $T_{\rm eff} = 9595$ K, and polar $\log g = 3.80$ for a fixed $V \sin i = 21.8$ km s^{-1}. In this case the mean values over the photosphere were $T_{\rm eff} = 9460$ K and $\log g = 3.78$, with equatorial minima of $T_{\rm eff} = 9325$ K and $\log g = 3.75$. The corresponding equatorial velocity was $V_{\rm rot} = 210$ km s^{-1} with a ratio of equatorial to polar radii of 1.028.

The result of the fit to the 4528–4530 Å region is shown in Figure 2, along with a best fit generated by assuming a slowly rotating, equator-on model for which $T_{\rm eff} = 9505$ K, $\log g = 3.69$, and $V \sin i = 23.7$ km s^{-1}. The difference in the quality of the fit is obvious; quantitatively the mean square deviation for the equator-on profile is 5.13×10^{-7}, double the 2.54×10^{-7} of the pole-on case. As predicted, Fe I λ4528 is a more sensitive discriminator than Ti II λ4529. Figure 2 also shows an equator-on profile generated by ROTATION with $T_{\rm eff} = 9550$ K, $\log g = 3.95$ (the CK model parameters) and $V \sin i = 21.8$ km s^{-1}. This equator-on model results in an even less satisfactory fit to the observations.

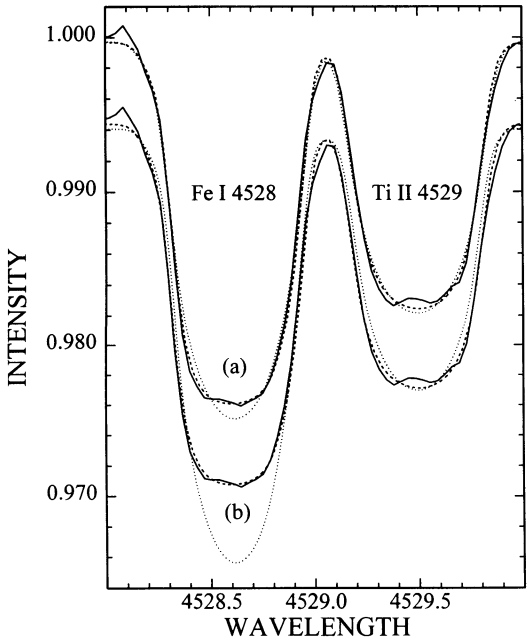

FIG. 2.—(*a*) Observed line profiles (*solid line*) for the 4528–4530 Å features due to Fe I λ4528 and Ti II λ4529. Also shown are the best fit for the rapidly rotating pole-on model (*dashed line*) with inclination 5°.1, polar $T_{\rm eff} = 9695$ K, $\log g = 3.75$, and $V \sin i = 21.8$ km s^{-1} and the best fit for a slowly rotating equator-on model (*dotted line*) with $T_{\rm eff} = 9540$ K, $\log g = 3.76$, and $V \sin i = 23.7$ km s^{-1}. (*b*) The same two profiles as in (*a*), plus the slowly rotating, equator-on model of Castelli & Kurucz (1994) (*dotted line*) with $T_{\rm eff} = 9550$ K, $\log g = 3.95$, and $V \sin i = 21.8$ km s^{-1}.

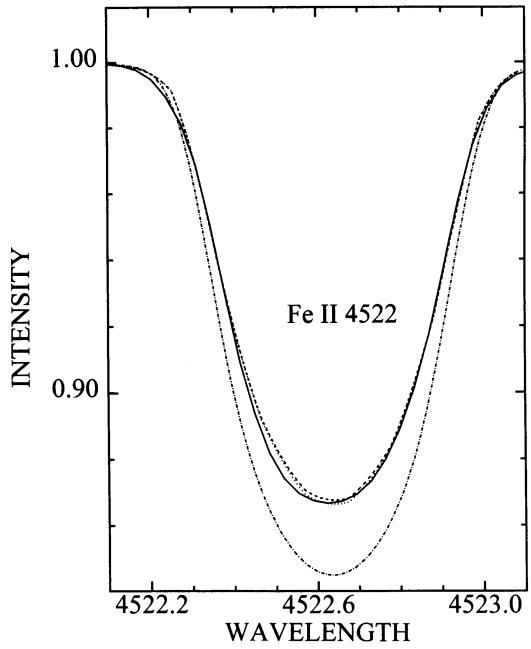

FIG. 3.—Observed Fe II λ4522 line profile (*solid line*) with the rapidly rotating pole-on model (*dashed line*) and two slowly rotating equator-on models, one with $T_{\rm eff} = 9500$ K, $\log g = 3.71$, $V \sin i = 22.6$ km s^{-1}, and $\xi = 1$ km s^{-1} (*dotted line*) and one using the model of Castelli & Kurucz (1994) with $\xi = 2$ km s^{-1} (*dash-dot line*).

To confirm that the pole-on model also reproduces the normal rotationally broadened profiles for other lines, Figure 3 shows the observed and calculated profiles for the unblended line Fe II λ4522. The calculated profiles are for the pole-on model and two equator-on models, the first generated by ROTATION with $T_{\rm eff} = 9500$ K, $\log g = 3.71$, $V \sin i = 22.6$ km s^{-1}, and $\xi = 1$ km s^{-1}, and the second generated by SYNTHE using the CK model parameters with $\xi = 2$ km s^{-1}. The pole-on model fits the observations very well except for the far wings and a thin section about -7 km s^{-1} from line center. The slight excess absorption in the wings is not an instrumental effect and, given its prevalence in other lines (Gulliver et al. 1991), must be intrinsic to the star. The feature to the blue of line center is also observed in the Fe II λ4520 and Ti II λ4534 profiles and could conceivably be due to an atmospheric anomaly. The equator-on, $\xi = 1$ km s^{-1} profile is very similar to the pole-on case, although slightly deeper. The equator-on model requires a larger $V \sin i$ to achieve the same broadening. The equator-on, $\xi = 2$ km s^{-1} profile is clearly unsatisfactory.

With the exception of the assumption that $V \sin i = 21.8$ km s^{-1}, an independent solution was determined by fitting the observed continuous flux H_ν in ergs cm^{-2} s^{-1} Hz^{-1} normalized to 1.0 at 5556 Å. The ultraviolet observations are from *IUE* as reported by Bohlin et al. (1990) from 1200 to 3300 Å, sampled at steps of 1.2 and 1.8 Å for the short- and long-wavelength ranges, respectively, with a resolution of about 6 Å. Internal standard deviations were 5.4% and 4.1%, respectively. From comparison with white dwarf model atmospheres, Bohlin et al. estimated systematic external errors in the *IUE*

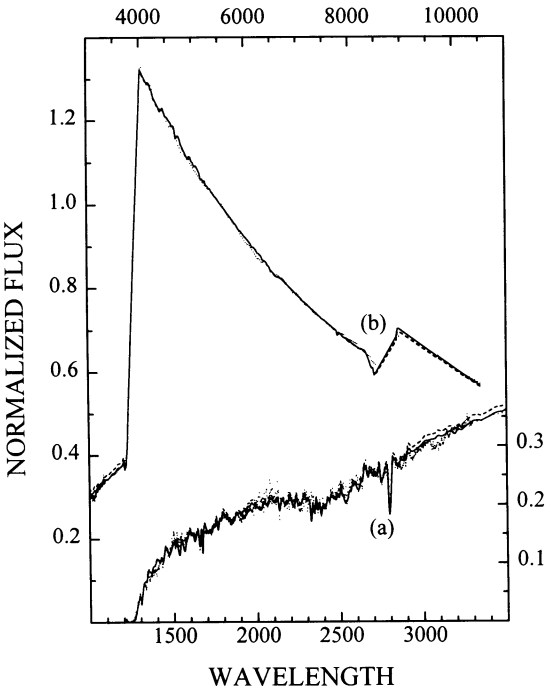

FIG. 4.—(*a*) Comparison of the ultraviolet *IUE* observations of Bohlin et al. (1990) (*dots*), the best-fit rapidly rotating pole-on model (*solid line*) for $V \sin i = 21.8$ km s^{-1}, inclination 6°.0, polar $T_{\rm eff} = 9595$ K, and log $g = 3.80$, and the Castelli & Kurucz (1994) model (*dashed line*). (*b*) Comparison of the continuum visual observations of Hayes (1985) (*dots*) and the same two models. The Balmer and Paschen lines have been removed throughout because of incompatibilities.

flux calibration to be less than 15%. It was necessary to scale the *IUE* flux values by a factor of 0.97 in the same manner as CK to agree with the visual observations at 3300 Å. The visual observations are the mean energy distribution of Hayes (1985) compiled from several sources and sampled at steps of 25 Å. The accuracy of the mean energy distribution is estimated by Hayes to be of order 1.0%–1.5%.

The best fit to the observed continuous spectrum from 1200–10,500 Å is shown in Figure 4 along with the CK model calculated using ATLAS9 and model data kindly supplied by F. Castelli. The quality of fit for the pole-on model is very good, with a mean square deviation of 8.05×10^{-5} over the entire range. For the CK model the mean square deviation is 1.08×10^{-4}, 35% higher. Visually the two models reproduce the observations equally well except in the region 2850–3700 Å, where the pole-on model has an advantage.

Of the two slightly different solutions presented here, that due to the line spectrum, inclination 5°.1, polar $T_{\rm eff} = 9695$ K, polar log $g = 3.75$, and $V \sin i = 21.8$ km s^{-1}, is deemed to be the better choice for two reasons. First, the quality of the data is better by more than an order of magnitude. Second, the line spectrum is more sensitive to the choice of model parameters. The determination of the errors which should be assigned to these four parameters is not straightforward. Although formal errors are calculated as part of the fitting process, their values of ±0°.3, ±25 K, ±0.02 dex, and ±0.2 km s^{-1}, respectively, are not believed to be realistic estimates. From the fine grid searches used to check for alternative solutions, more conservative error estimates for the line spectrum are ±0°.5, ±25 K, ±0.05 dex, and ±0.2 km s^{-1}, respectively. Realistic errors for the continuous spectrum are estimated at double these values. Within these errors both solutions are in agreement.

Although the mean $T_{\rm eff} = 9500 \pm 25$ K is in good agreement with the best fit $T_{\rm eff} = 9550$ K of CK, the mean log $g = 3.71 \pm 0.05$ is significantly different from the best fit log $g = 3.95$ of CK. Since an excellent fit is achieved to both spectral lines and a very similar solution is found for the continuous spectrum, it is not possible to attribute this difference in log g to any error in the line parameters, say, for example, the *gf*-value for either line. Of course log g is normally determined by a fit to the observed Hα, Hβ, and Hγ profiles of Peterson (1969). This method is now being pursued using ROTATION.

We thank James E. Hesser, Director of the Dominion Astrophysical Observatory, for the observing time; Robert L. Kurucz for the use of ATLAS9 and SYNTHE programs; Fiorella Castelli for providing us with a preprint of the paper on model atmospheres of Vega, George W. Collins and Richard O. Gray, for useful discussion, as well as an anonymous referee for several important suggestions and criticisms. Financial support for part of this work was provided to A. F. G. by the National Sciences and Engineering Research Council of Canada and to S. J. A. by NASA grant NAG 5-1551 to The Citadel and by grants from the Citadel Development Foundation.

REFERENCES

Adelman, S. J. 1988, MNRAS, 230, 671
Adelman, S. J., & Gulliver, A. F. 1990, ApJ, 348, 712
Aumann, H. H., et al. 1984, AJ, 96, 1415
Bevington, P. R. 1969, Data Reduction and Error Analysis for the Physical Sciences (New York: McGraw-Hill)
Bohlin, R. C., Harris, A. W., Holm, A. V., & Gry, C. 1990, ApJS, 73, 413
Castelli, F., & Kurucz, R. L. 1994, A&A, 281, 817 (CK)
Collins, G. W. 1963, ApJ, 138, 1134
Elste, G. H. 1992, ApJ, 384, 284
Fletcher, J. M. 1990, private communication
Fuhr, J. R., Martin, G. A., & Wiese, W. L. 1988, J. Phys. Chem. Ref. Data, 17, Suppl. 4
Gray, R. O. 1985, JRASC, 79, 237
———. 1988, JRASC, 82, 336
Gulliver, A. F., Adelman, S. J., Cowley, C. R., & Fletcher, J. M. 1991, ApJ, 380, 223
Hanbury Brown, R., Davis, J., Allen, L. R., & Rome, J. M. 1987, MNRAS, 137, 393
Hayes, D. S. 1985, in Calibration of Fundamental Stellar Quantities, ed. D. S. Hayes, L. E. Pasinetti, & A. G. D. Philip (Dordrecht: Reidel), 225
Hill, G. 1979, Publ. Dominion Astrophys. Obs., 15, 297
———. 1986, LIGHT2 User Manual
Kurucz, R. L. 1993, ASP Conf. Ser. 44, Peculiar versus Normal Phenomena in A-Type and Related Stars, ed. M. M. Dworetsky, F. Castelli, & R. Faraggiana (San Francisco: ASP), 87 (see also CD-ROM distribution)
Kurucz, R. L., & Avrett, E. H. 1981, Smithsonian Astrophys. Obs. Spec. Rep., No. 391
Martin, G. A., Fuhr, J. R., & Wiese, W. L. 1988, J. Phys. Chem. Ref. Data, 17, Suppl. 3
Peterson, D. M. 1969, Smithsonian Astrophys. Obs. Spec. Rep., No. 293